International Journal of Nanoelectronics and Materials
Volume 14 (Special Issue) August 2021 [241-262]

Prediction of Basic and Circular Vibration Isolator in High Frequencies using Malaysian Natural Rubber for Highway C2L Machine

Mohd Azli Salim[1,2,3*], Adzni Md. Saad[1,3], Feng Dai[4], Norbazlan Mohd Yusof[5], Nurfaizey Abdul Hamid[1] and Nor Azmmi Masripan[1,2,3]

[1]Fakulti Kejuruteraan Mekanikal, Universiti Teknikal Malaysia Melaka, Hang Tuah jaya, 76100 Durian Tunggal, Melaka, Malaysia
[2]Advanced Manufacturing Centre, Universiti Teknikal Malaysia Melaka, Hang Tuah Jaya, 76100 Durian Tungggal, Melaka, Malaysia
[3]Intelligent Engineering Technology Services Sdn. Bhd., No.1, Jalan TU43, Taman Tasik Utama, 76450 Ayer Keroh, Melaka, Malaysia
[4]Institute of Science and Technology, China Railway Eryuan Engineering Group Co.Ltd, No.3 Tongjin Road, Sichuan, 610031, P.R.China
[5]Menara Korporat, Persada PLUS, Persimpangan Bertingkat Subang, KM15, Lebuhraya Baru Lembah Klang, 47301, Petaling Jaya, Selangor, Malaysia

ABSTRACT

This paper represents the basic and circular vibration isolator in High Frequencies using Malaysian natural rubber. Rubber material is chosen because it has very high damping to ensure the sufficient dissipation of vibration energy from the seismic wave. They are two methods involve in this paper, which are lumped parameter and wave propagation techniques. The lumped parameter system is developed to represent the baseline model of laminated rubber-metal spring. Wave propagation model is developed using non-dispersive rod. The mathematical modeling of laminated rubber-metal spring has been developed based on the internal resonance, lumped parameter and finite rod model, respectively. For a conclusion, the mathematical modeling of a prediction of basic and circular vibration isolator can be as a tool to predict the new trial-error method for developing new compounding of the vibration isolator in future, respectively.

Keywords: Laminated rubber-metal spring, vibration isolator, Malaysian natural rubber, internal resonance, transmissibility

1. INTRODUCTION

Rubber bearing has been widely used as an isolator to suppress the level of vibration, especially in building structures for earthquake protection. It is made from layers of rubber with thin steel plates between them, and a thick plate located at the top and the bottom of the rubber materials. These rubber bearings are located between the bottom of a building and its foundation. By embedding the metal plates, the combination provides better performance in terms of stress and strain level when a heavy load is applied and prevents a bulging effect in the horizontal direction [1]. It is also designed to be very stiff and strong for vertical load; therefore, it can carry the heavy weight of the building. Imbimo and Luca (1998) studied the rubber bearings to investigate the effect of the shape factor on the stress distributions and stress concentration of the natural rubber (NR) elastomer subjected to longitudinal load [2].

In this study, the finite element analysis (FEA) approach was used to produce an approximated solution. The numerical results found in this study were then compared with an analytical approximated solution. Based on this comparison study, it was found that a beneficial effect of

*Corresponding Author: azli@utem.edu.my

the shape factor was higher stress distribution and stress concentration parallel with the reduction of edge effects. In 2007, this study was followed by other researchers who studied the use of rubber bearings to support bridges being built as part of new highway construction in Greece [3-5]. Two samples of rubber bearings were located at the bridge columns. The test results showed that the stiffness and damping ratio had a good relationship with longitudinal load as well as the frequency of the horizontal displacement. The total displacement of the rubber bearings was proportional to the force applied to them. Figure 1.1 shows the dynamic model proposed by Manos of an isolated bridge structure. It was found that, by employing the isolation strategy, the superstructure motion was decoupled from the pier's motion during an earthquake. The inertia forces could be reduced and at the same the energy was dissipated by the vibration isolators, which, finally, reduced the acceleration transmitted into the superstructure.

Bhuiyan (2010) modelled the hysteretic behaviour of rubber bearings under uni-directional horizontal displacement and constant horizontal compressive load [6]. Three types of bearing were used in these studies, namely NR bearing, lead rubber bearing and high-damping rubber bearing. Several experiments were conducted to analyse the performance of the bearings, such as basic test, multi-step relaxation, cyclic test and simple relaxation. It was found that the NR bearings gave the best result in terms of the rate-dependent rheology. This represents the typical shear stress-strain responses of high-damping rubber bearings where the strain rate dependency of hysteresis occurs.

Most recently, rubber bearings had successfully been applied in construction of Penang Second Bridge in Penang, Malaysia. Incorporation of the bearings mainly aimed to avoid the effects arising from the natural environment, such as earthquakes and ocean waves. Figure 1 shows the overall view of Penang Second Bridge and Figure 2 shows the location of the rubber bearings in the bridge.

Figure 1. Overall view of Penang second bridge.

Figure 2. Location of the rubber bearings in Penang second bridge.

The rubber bearings in Penang Second Bridge were designed to shift the fundamental resonant frequency of the bridge away from earthquake ground motion frequencies. Several studies had been conducted before, including the quasi-static, static, dynamic and elastomer tests. Based on the quasi-static and dynamic tests, a rubber-bearing prototype was developed and a bi-longitudinal test was carried out in the longitudinal direction. Compression-shear tests in double shear configuration were also conducted to investigate the shear stiffness and damping ratio. If the results obtained did not meet the standards used for Penang Second Bridge, a new prototype was developed with new formulations. In the elastomer test, each compound was tested according to the international standard developed by Lembaga Getah Malaysia (LGM). A similar trial-error approach was applied where a new compound would be redesigned to ensure that the requirements were fulfilled.

Therefore, this paper represents the prediction of the basic and circular vibration isolator in high frequencies using Malaysian NR. At the end of the study, it hopes the prediction can be as a tool to predict the new trial-error method for developing new compounding of the vibration isolator, respectively.

2. MODELLING OF LUMPED PARAMETER SYSTEM

Theory of vibration isolator is developed from elastic springs and viscous damping, which is called a lumped parameter system. This system is presumed to be massless for convenience in the modelling process.

In this section, the vibration isolator is modelled using a lumped parameter system consisting of mass, damper and spring components. To assess the vibration isolation performance, the spring is loaded with a lumped mass M excited together with a harmonic force F_e . The rubber is ideally modelled as a massless component having a constant stiffness k and damping coefficient c . The embedded plate is treated as a rigid solid mass m without damping and stiffness. The laminated rubber-metal spring (LR-MS) model is attached to a rigid structure and the transmissibility is derived. Vertical motion is the only input that taken into account. Here, the rotational motion is neglected. Figure 3 shows the schematic diagram of the LR-MS model with one layer of metal plate, which creates a two-degree-of-freedom system.

Two equations of motion can be derived as follows

$$M\ddot{u}_1 + c_1(\dot{u}_1 - \dot{u}_2) + k_1(u_1 - u_2) = F_e \tag{1}$$

and

$$m\ddot{u}_2 + c_1(\dot{u}_2 - \dot{u}_1) + c_2\dot{u}_2 + k_1(u_2 - u_1) + k_2u_2 = 0 \tag{2}$$

where, u_1 is the displacement of loaded mass and u_2 is the displacement of the embedded plate.

Due to a harmonic force, the resulting motion of the system is also harmonic. Substituting $u = Ue^{j\omega t}$ in Eq. (1) and Eq. (2) with U the complex amplitude and ω the frequency, the equations of motion can be expressed in matrix form as

$$\left(-\omega^2\begin{bmatrix} M & 0 \\ 0 & m \end{bmatrix} + j\omega\begin{bmatrix} c_1 & -c_1 \\ -c_1 & c_1 + c_2 \end{bmatrix} + \begin{bmatrix} k_1 & -k_1 \\ -k_1 & k_1 + k_2 \end{bmatrix}\right)\begin{Bmatrix} U_1 \\ U_2 \end{Bmatrix} = \begin{Bmatrix} F_e \\ 0 \end{Bmatrix} \tag{3}$$

or in general form

$$[-\omega^2\mathbf{M} + j\omega\mathbf{C} + \mathbf{K}]\tilde{\mathbf{U}} = \tilde{\mathbf{F}} \tag{4}$$

where **M** is the mass matrix, **C** is the damping matrix, **K** is the stiffness matrix, and $\tilde{\mathbf{U}}$ and $\tilde{\mathbf{F}}$ are the vectors of complex displacement amplitude and force, respectively.
The displacements u_1 and u_2 at each frequency ω can therefore be obtained by

$$\tilde{\mathbf{U}} = [-\omega^2\mathbf{M} + j\omega\mathbf{C} + \mathbf{K}]^{-1}\tilde{\mathbf{F}} \tag{5}$$

where $\mathbf{A}^{-1}$ indicates the inverse of matrix **A**.

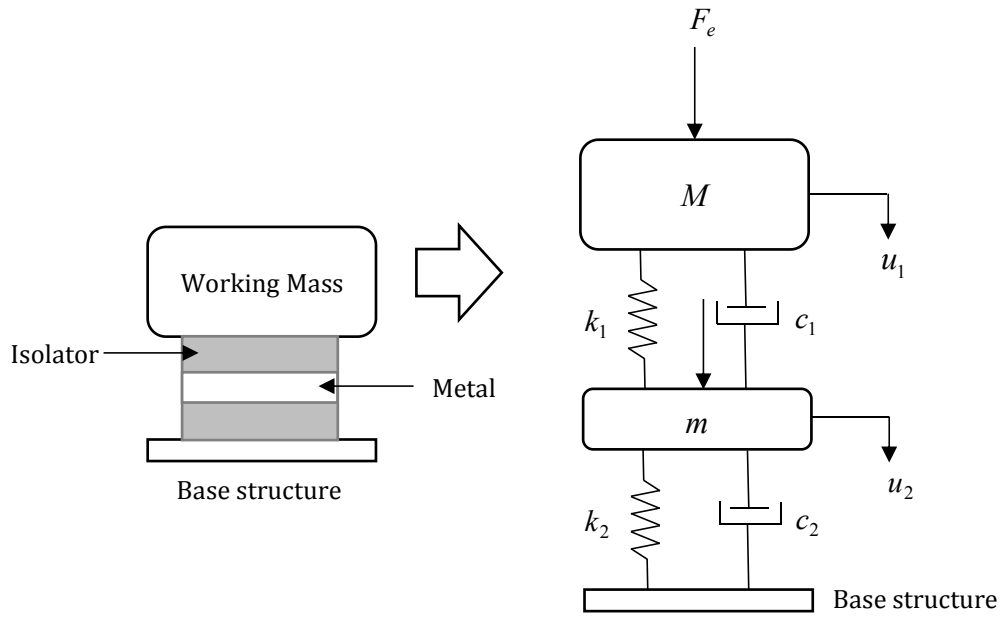

Figure 3. Mass-damper-spring model of a lumped parameter system.

For the case of the model in Figure 3, the force transmitted to the base structure can be written as a function of the displacement of the bottom metal layer.

For an excitation force of unit amplitude $F_e = 1$, the transmissibility, i.e. the amplitude ratio of transmitted force to excitation force, is thus given by

$$T = \left|\frac{F_t}{F_e}\right| = \left|F_t\right| = U_2\sqrt{(k_2^2 + \omega^2 c_2^2)} \tag{6}$$

For two layers of metal plates inside the rubber blocks (three-degree-of-freedom system), the mass, damping and stiffness matrices in Eq. (4) are given by

$$\mathbf{M} = \begin{bmatrix} M & 0 & 0 \\ 0 & m_1 & 0 \\ 0 & 0 & m_2 \end{bmatrix}, \mathbf{C} = \begin{bmatrix} c_1 & -c_1 & 0 \\ -c_1 & c_1 + c_2 & -c_2 \\ 0 & -c_2 & c_2 + c_3 \end{bmatrix} \text{ and } \mathbf{K} = \begin{bmatrix} k_1 & -k_1 & 0 \\ -k_1 & k_1 + k_2 & -k_2 \\ 0 & -k_2 & k_2 + k_3 \end{bmatrix} \tag{7}$$

By observing the structural pattern of the matrices in Eqs. (3), (4) and (7), for N layers of metal plates, the matrices thus have dimensions of $(N+1)\times(N+1)$ and are expressed as

$$\mathbf{M} = \begin{bmatrix} M & 0 & 0 & 0 \\ 0 & m & 0 & 0 \\ \vdots & \cdots & \ddots & \vdots \\ 0 & \cdots & 0 & m_N \end{bmatrix}, \mathbf{C} = \begin{bmatrix} c_1 & -c_1 & 0 & 0 & \cdots & 0 \\ -c_1 & c_1 + c_2 & -c_2 & 0 & \cdots & 0 \\ 0 & -c_2 & c_2 + c_3 & -c_3 & \cdots & \vdots \\ \vdots & \vdots & \vdots & \vdots & \ddots & c_N \\ 0 & 0 & \cdots & -c_{N-1} & & c_{N-1} + c_N \end{bmatrix},$$

$$\mathbf{K} = \begin{bmatrix} k_1 & -k_1 & 0 & 0 & \cdots & 0 \\ -k_1 & k_1 + k_2 & -k_2 & 0 & \cdots & 0 \\ 0 & -k_2 & k_2 + k_3 & -k_3 & & \vdots \\ \vdots & \vdots & & & \ddots & k_N \\ 0 & \cdots & \cdots & 0 & -k_{N-1} & k_{N-1} + k_N \end{bmatrix}$$

and

$$\widetilde{U} = \{u_1 \quad u_2 \quad \cdots \quad \cdots \quad u_{N-1}\}^T, \ \widetilde{F} = \{F_e \quad 0 \quad \cdots \quad \cdots \quad 0\}^T \tag{8}$$

Figures 4 to 8 plot the transmissibility for different numbers of layers *N* of embedded metal plates. The calculation is made assuming the mass of each plate is the same as the loaded mass. This assumption is important to make the masses of the metal plates are evenly distributed along the isolators, and the position always remain the same during apply the huge loaded mass at the top of the isolator. The damping is also assumed to be very small. Peaks indicating amplification of the injected force to the received structure can be seen at low frequencies, for example at 10 Hz, which appear at the natural frequencies of the system where length $L = 0.14$ m, outer radius $R = 0.05$ m, inner radius $r = 0.005$ m, Young's modulus $E = 1.4$ MPa and density $\rho = 920$, respectively By embedding more plates in the rubber, the higher the number of degree-of-freedom and more natural frequencies the system has. Note that the total length of the isolator for lumped parameter system is kept constant. Therefore, if N number of masses from metal plates are added, the length of the isolator becomes $L/(N+1)$, which then reduces the stiffness of each element of the isolator. In consequence, increases the internal natural frequencies of the lumped parameter system apart from the fundamental frequency.

It can be seen that the resonance peaks appear in the isolation frequency area at roughly 20 Hz, which degrades the isolation performance of the vibration isolators, and it started from four metal plates, three metal plates and lastly one metal plates, respectively. It is interesting to observe that the transmissibility curve rapidly decreases with the increase in the number of embedded metal plates in the natural rubber above 100Hz. It happens because the damping of the metal plate effect is reversed in the isolation region, and by increasing the damping in the natural rubber, it was detrimental to the performance in the isolation region.

Additionally, these results are from the lumped parameter modelling in the form of transmissibility F_t/F_e . The transmissibility curve is started at unity at low frequencies indicating the initial excitation force. Then, the curve is continuously increasing and the highest peak is located at 10 Hz, and finally it can be seen reduced below unity until 3000 Hz. However, it is interesting to observe that the transmissibility curve rapidly decreases with the increased number of embedded metal plates in the rubber above 100 Hz.

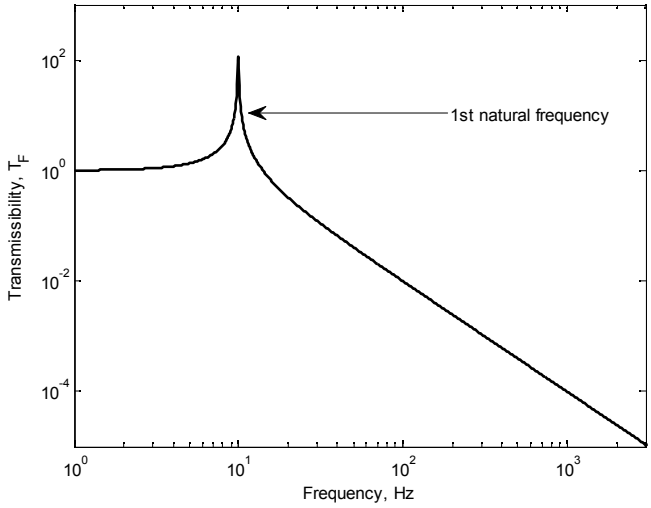

Figure 4. Lumped parameter system without a metal plate.

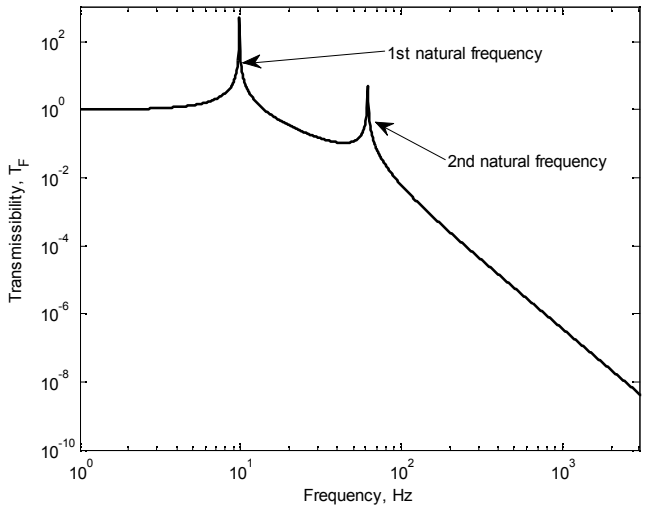

Figure 5. Lumped parameter system with a single metal plate.

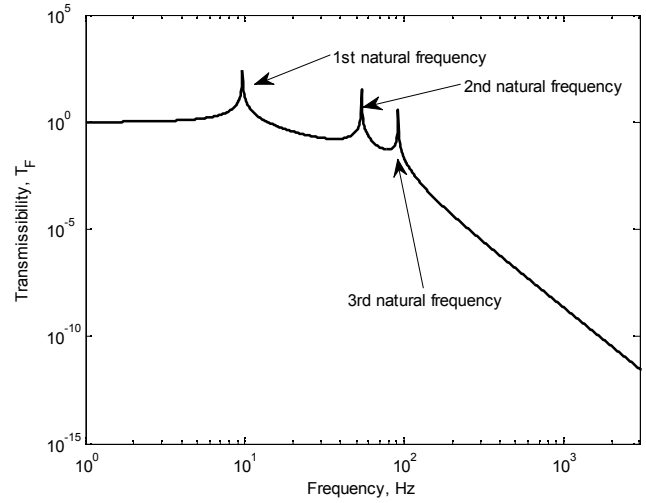

Figure 6. Lumped parameter system with two metal plates.

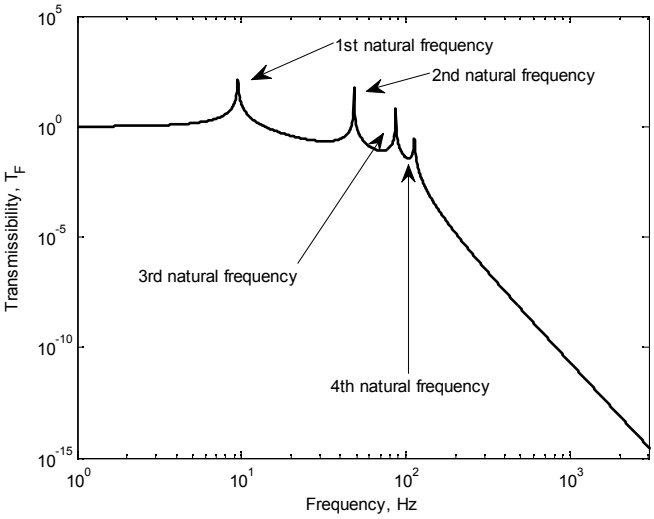

Figure 7. Lumped parameter system with three metal plates.

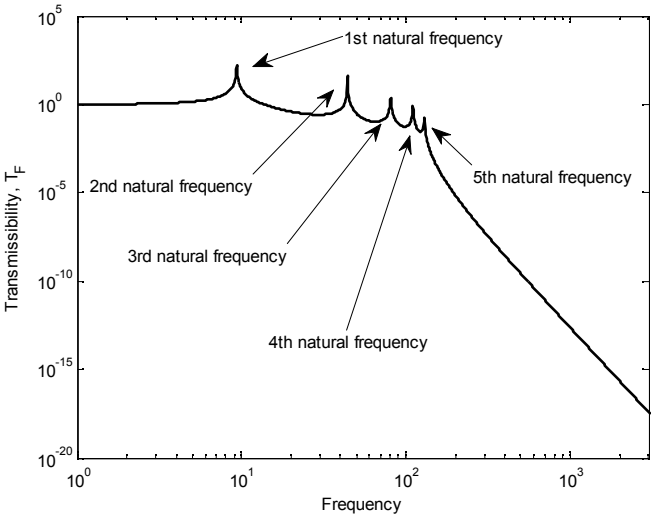

Figure 8. Lumped parameter system with four metal plates.

Figure 9 shows the schematic diagram of vibration isolators which is presented as a lumped parameter system. Then, Figure 10 shows the transmissibility results for the lumped parameter system with and without a metal plate in one plot. This indicates that the lumped parameter system improves the vibration isolation at high frequency.

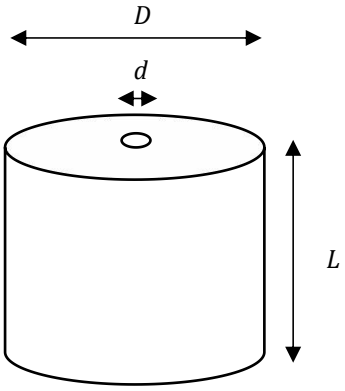

Figure 9. Schematic diagram of vibration isolators: *D* is outer diameter, *d* is inner diameter and *L* is total length of the isolator.

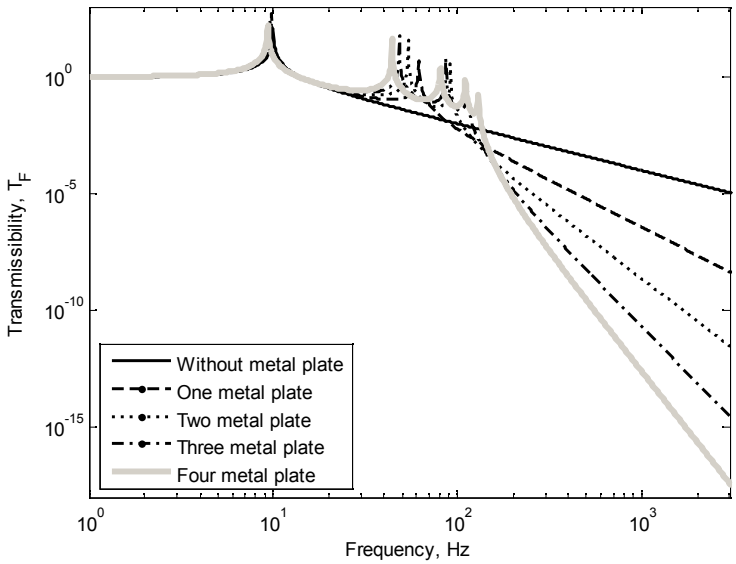

Figure 10. Combined results for lumped parameter systems.

However, this lumped parameter system model ignores the mass of the rubber which can contribute to more internal resonances. Besides that, the reason to ignore the mass of the rubber is because in reality, it is not relevant to compare the isolators mass with the huge working load, and furthermore the ratio is too small. The width of the rubber layer is neglected as, at high frequencies when the wavelength is much smaller than the rubber layer thickness, wave effects from various directions affect the isolation performance.

Additionally, the application of the lumped parameter system in this section was limited to frequencies less than 3000 Hz due to a lack of versatility, and potentially the performance of the system. Besides, there are significant limitations for application of four metal plate in structural applications, where broadband disturbances of highly uncertain nature can be countered. Then, the wave effect has been highlighted in the classical rubber rod isolator.

3. WAVE EFFECTS IN VIBRATION ISOLATION

Vibration isolators that can be used in higher frequencies range must have distributed mass, stiffness and damping. These three properties are important to investigate the dynamic behaviours of vibration isolators. For the elastic motion of vibration isolators, these dynamic behaviours merge with resonance behaviour, and finally create various number of frequencies, and these represent the natural mode of the vibration isolator. Many researchers agree that the resonance behaviour occurs in vibration isolators due to wave effects, and it is known as internal resonances [7].

There have been many discussions about this issue and one of the conclusion that can be made is that internal resonance is determined by several factors such as material properties, dimensions, boundary conditions, shape, deformation, shear, tension, compression and many more [8]. In general, the wave effect occurs in heavy and larger vibration isolators. This is because small vibration isolators only have static stiffness, which does not influence the internal resonance. When internal resonance occurs in a vibration isolator in some frequency ranges, the wavelength of the vibration isolator can be measured and can be compared with the original length of the vibration isolator. Based on previous studies, it can be stated that the wavelength will decrease when the frequency ranges increase, and it reveals that, in high frequency ranges, the internal resonance occurs automatically [9-10].

Generally, heavy instruments or machinery in industry operate at high speeds, which potentially create many problems in terms of vibration level. Vibration isolation is proposed to be used to avoid the vibration energy being transferred to the environment, especially to building structures. This situation is crucial during high frequency, and the selection of the vibration isolation must be done correctly.

To solve this problem, the idea of a finite rod model has been developed to observe the wave effects in a vibration isolator; it has a simple shape and can also be modelled as an elastic finite rod [8]. The properties of the finite rod model consist of internal damping and the mass, depending on the material density. A finite rod model is developed following the distributed parameter isolator models, which means conventionally it is a single-degree-of-freedom of a passive vibration isolation system. This model is able to overcome the high frequency ranges issue because, even if the internal resonances reach high frequencies, the transmissibility of the finite rod model will not be reduced when the frequency reaches the resonance limit because it is one of the versatile and adaptable materials. Additionally, it is able to withstand large strains and can store more elastic energy, besides, it possesses some inherent damping which is given benefit for the materials when resonance. The bulk modulus of the rubber is high, and it can be remained to prevent changes in shape and become much stiffer.

From previous investigation, the initial transmissibility of the finite rod model is only 20 dB per decade, which is less than twice of the massless model. Apart from that, in the finite rod model the lateral deformation on longitudinal excitation can be avoided. By using this model, it can be observed that the quantum of amplitude for internal resonances is reduced by decreasing the frequency ranges. In this model, one simple conclusion has been made, which is that it is important to know the first few peaks of internal resonance in order to establish the performance of the vibration isolator, and this is in agreement with the view of a previous researcher [11].

3.1 Mathematical Modelling of Wave Effects using Wave Propagation Method

Wave-based method has been developed in order to enhance the prediction tools, and also increase the computational efficiency, thus it can extend the applicability to evaluate and determine the models in higher frequencies range. Most of the researchers presume that the

waveguide properties in wave-based method are homogeneous due to the direction of the travelling wave. It limits the application of the method itself. Analytical approach for non-homogenous waveguides, such as ducts, acoustic noise, rod, beam and many more cannot be applied. Therefore, approximation of the wave solution is used along with the generalized method for one-dimensional waveguides in term of propagation known as wave propagation method. This method requires the internal reflection wave in order to neglect local changes due to material and geometrical properties. Additionally, this method is used to derive the mathematical expressions for natural frequencies and input mobility of finite length waveguides. Besides, it can be included in the formulation straightforwardly, and the mathematical expression of the expansion can be used to develop the approximation form of the natural frequencies for rods and beams.

In the next section, the wave effect is derived using wave propagation method of forced vibration response for a rod as an example. A formulation in term of propagation and dynamic stiffness matrix in longitudinal vibration is presented in details.

3.2 Wave Effects in Longitudinal Vibration

There has been increasing interest in investigating the longitudinal vibration [11]. The finite rod model, also known as the non-dispersive finite rod model, is one of the examples of this elastic body. Most studies of the longitudinal wave have only been carried out on the longitudinal direction and have neglected any lateral contraction on expansion of the rod. This theory is an approximation based on the strength of materials theory. Several studies have produced an approximation theory and the results can be concluded as being very good if the wavelengths of the motion are long compared to the rod's cross-sectional dimension. In addition, plane cross-sections of the rod remain as a plane and parallel during deformation by the wave propagation method.

The aim of this section is to evaluate the characteristics of internal resonance in a non-dispersive finite rod for a single-degree-of-freedom system in a longitudinal direction. Consider now the isolator as a rubber block forming the shape of a uniform cylindrical block having length L subjected to an longitudinal force with amplitude F_e, as shown in Figure 11.

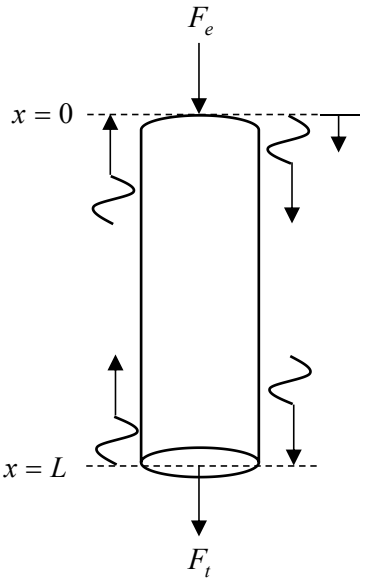

Figure 11. Uniform non-dispersive finite rod undergoing longitudinal force.

The longitudinal wave is assumed to propagate along the length of the non-dispersive finite rod, and for harmonic excitation at frequency ω the displacement can be written as

$$u(x,t) = U(x)e^{j\omega t} = \left(Ae^{jk_l x} + Be^{-jk_l x}\right)e^{j\omega t} \tag{9}$$

where A and B are the complex wave amplitudes and the $k_l = \omega/c_l$ is the longitudinal wavenumber where $c_l = \sqrt{E(1+j\eta)/\rho}$ is the longitudinal wave speed with E the Young's Modulus and ρ the density.

Note that damping has been introduced in the Young's modulus E where η is the damping loss factor. The impedance at a particular location can be obtained by unrestraining the motion at which force is applied, but restraining the motion elsewhere.

The point localized impedances at each end of the isolator (at $x = 0$ and $x = L$) are

$$Z_{11} = \left.\frac{F_e}{\dot{u}(0)}\right|_{\dot{u}(L)=0} = \left.\frac{F_e}{j\omega u(0)}\right|_{\dot{u}(L)=0} \tag{10}$$

and

$$Z_{22} = \left.\frac{F_t}{\dot{u}(L)}\right|_{\dot{u}(0)=0} = \left.\frac{F_t}{j\omega u(L)}\right|_{\dot{u}(0)=0} \tag{11}$$

where $\dot{u} = du/dt$.

From Hooke's Law at $x = 0$ where $\partial u(0)/\partial x = -F_e/\kappa_l$, Eq. (9) gives

$$A - B = \frac{jF_e}{\kappa_l k_l} \tag{12}$$

where $\kappa_l = E(1+j\eta)S$ is the longitudinal rigidity and S is the cross-sectional area of the non-dispersive finite rod.

From the boundary condition in Eq. (10) at $x = L$ when $u(L) = 0$ yields (Yan, 2007)

$$B = -Ae^{2jk_l L} \tag{13}$$

By substituting Eq. (3.13) into Eq. (3.12) yields

$$A = \frac{jF_e}{k_l \kappa_l}\left(\frac{1}{e^{2jk_l L}+1}\right) \tag{14}$$

and

$$B = \frac{-jF_e}{k_l \kappa_l}\left(\frac{e^{2jk_l L}}{e^{2jk_l L}+1}\right) \tag{15}$$

From the boundary condition stated in Eqs. (10) and (11), the displacement at $x = 0$ is

$$u(0) = A + B = \frac{F_e}{jk_l \kappa_l}\left(\frac{e^{2jk_l L}-1}{e^{2jk_l L}+1}\right) = \frac{F_e}{k_l \kappa_l}\tan(k_l L) \tag{16}$$

Applying the principle of reciprocity, where $Z_{11} = Z_{22}$, the point impedances in Eq. (10) and Eq. (11) are thus given by

$$Z_{11} = Z_{22} = \frac{F_e}{j\omega u(0)} = \frac{k_l \kappa_l}{j\omega \tan(k_l L_l)} = \frac{S\sqrt{E\rho}}{j\tan(k_l L)} \tag{17}$$

The transfer impedance is defined by restraining the location where the force is applied and unrestraining the other end of the rod. It is written as

$$Z_{12} = \left.\frac{F_e}{\dot{u}(L)}\right|_{\dot{u}(0)=0} \tag{18}$$

and

$$Z_{21} = \left.\frac{F_t}{\dot{u}(0)}\right|_{\dot{u}(L)=0} \tag{19}$$

From Eq. (10) and Eq. (11), where $\dot{u}(0) = 0$, this yields $A = -B$. Substituting this to Eq. (12) gives

$$A = \frac{F_e}{2jk_l \kappa_l} \tag{20}$$

and

$$B = \frac{-F_e}{2jk_l \kappa_l} \tag{21}$$

Substituting Eq. (20) and Eq. (21) into Eq. (9), the displacement at the end of the isolator i.e. at $x = L$ can be given by

$$u(L) = \frac{F_e}{2jk\kappa}\left(e^{-jk_l L} - e^{jk_l L}\right) = \frac{-F_e}{k_l \kappa_l}\sin(k_l L) \tag{22}$$

Again, from the principle of reciprocity where $Z_{21} = Z_{12}$, the transfer impedance in Eq. (18) and Eq. (19) is

$$Z_{21} = Z_{12} = \frac{F_e}{j\omega u(L)} = \frac{-k_l \kappa_l}{j\omega \sin(k_l L)} = \frac{-k_l S\sqrt{E\rho}}{j\sin(k_l L)} \tag{23}$$

Note that here the damping is assumed to be very small, i.e. $\eta << 1$.

The impedance for the non-dispersive finite rod due to longitudinal waves can therefore be written in matrix form as

$$Z = \begin{bmatrix} Z_{11} & Z_{12} \\ Z_{21} & Z_{22} \end{bmatrix} = \frac{k_l \kappa_l}{j\omega \sin(k_l L)} \begin{bmatrix} \cos(k_l L) & -1 \\ -1 & \cos(k_l L) \end{bmatrix} \tag{24}$$

or

$$Z = \frac{S\sqrt{E\rho}}{j\sin(k_l L)} \cdot \begin{bmatrix} \cos(k_l L) & -1 \\ -1 & \cos(k_l L) \end{bmatrix} \tag{25}$$

With the stiffness defined as $K = j\omega Z$, the stiffness matrix from Eq. (24) is therefore

$$K = \begin{bmatrix} K_{11} & -K_{12} \\ -K_{21} & K_{22} \end{bmatrix} = \frac{\omega S\sqrt{E\rho}}{\sin(k_l L)} \cdot \begin{bmatrix} \cos(k_l L) & -1 \\ -1 & \cos(k_l L) \end{bmatrix} \tag{26}$$

4. INTERNAL RESONANCE BEHAVIOUR IN RODS

The longitudinal waves of the impedances of $Z_{11} = Z_{22}$ and $Z_{12} = Z_{21}$ are shown in Figure 12. These are plotted for length $L = 0.14$ m, outer radius $R = 0.05$ m, inner radius $r = 0.005$ m, Young's modulus $E = 1.4$ MPa and density $\rho = 920$, respectively. According to these figures, the internal resonance waves for both results started at 68 Hz and fluctuated until high frequency was reached. Two patterns of internal resonance wave occurred in the longitudinal system; one is from the positive wave and the other one is from the opposite direction. For the impedance matrix, the wave starts at point 1×10^4, which represents the impedance value of the system itself. However, the value of impedance rapidly decreases associated with the increase of frequency. The fluctuated wave is huge between the range of 68 Hz to 105 Hz and it is slowly stabilised with the increase of frequency. According to this figure, the internal resonance for the impedance matrix occurs to a greater degree only at certain frequencies. Besides, it can be seen that the wave occurred in higher frequencies, when the wavelength of the rod is comparable with the rod's length. Thus, the wavelength is inversely proportional to the frequency, and finally, it is occurred at high frequencies.

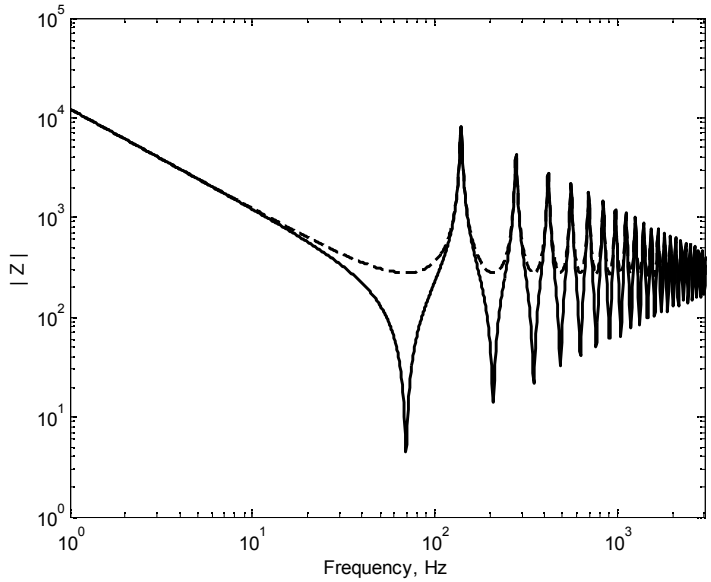

Figure 12. Longitudinal wave for impedance: - $Z_{11} = Z_{22}$, --- $Z_{12} = Z_{21}$.

Figure 13 shows the internal resonance in the stiffness matrix. The starting point of internal resonance is located at 7×10^5 , where this value represents the total amount of stiffness of the non-dispersive finite rod in the longitudinal condition. The wave fluctuations start constantly at 68 Hz in a sinusoidal pattern, but the amplitude rapidly decreases with the increase of frequency. There is a reasonably close relation of the internal resonance pattern between these two matrices, but from an analytical approach it is totally different.

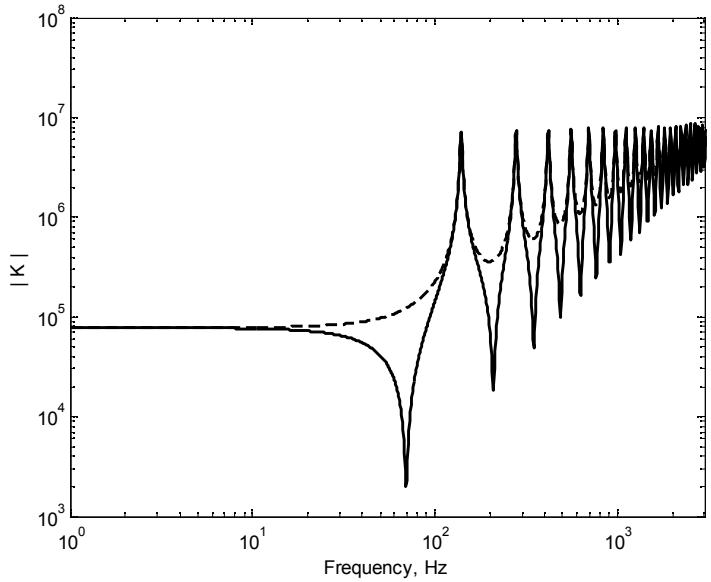

Figure 13. Longitudinal wave for stiffness: - $K_{11} = K_{22}$, --- $K_{12} = K_{21}$.

4.1 Distributed Parameter Isolator

As described in previous section, for conventional vibration isolators, in which the mass of isolator is assumed to be neglected, the information about isolators' basic guidelines for designing new isolators is offered. But according to previous researchers, this assumption is not

valid for higher frequencies because the wavelength of the isolator is long compared to its actual size. At higher frequencies, the predictions by using massless vibration isolators are no longer accurate, and finally it will mislead the internal resonances effect. Therefore, the distributed parameter isolator is introduced which has distributed mass, stiffness and damping [12-13].

In this section, the distributed parameter isolator undergoing base motion are investigated. Additionally, the performance of the vibration isolator in isolating the vibration energy transmitted to the mass is also assessed. In general, distributed parameter isolator models can be divided into two categories for the purposes of dynamic investigation. The first category can be derived using second-order partial differential equations (PDEs) and it is called a non-dispersive isolator, where the wave speed of the isolator is independent of the frequency. The second category can be modelled using fourth or higher order PDEs and it is known as a dispersive isolator, and the wave speed is dependent on the frequency range.

The distributed parameter isolator is modelled as a non-dispersive finite rod under longitudinal vibration and it is called a laminated rubber-metal spring. Figure 14 shows the schematic diagram of the basic model of the LR-MS. It consists of alternating layers of vulcanized natural rubber (NR) reinforces by a metal plate. The basic element of LR-MS model is NR layers laminated in the middle by a metal plate.

Figure 15 illustrates the schematic diagram for a non-dispersive finite rod where the excitation force F_e is generated by applying mass M at the top of the non-dispersive finite rod, and F_t is the transmitted force. The working mass M represents a total mass effect from preload to the laminated layer and metal plates. The wave effect equation for a one-dimensional element for the non-dispersive finite rod was derived in Section 3.3 and the equation was represented in matrix form.

Basically, the impedance method was used more than 10 years ago, and the purpose of the study is to identify the relationship between electrical-mechanical properties or to simplify the mechanical system's formulation.

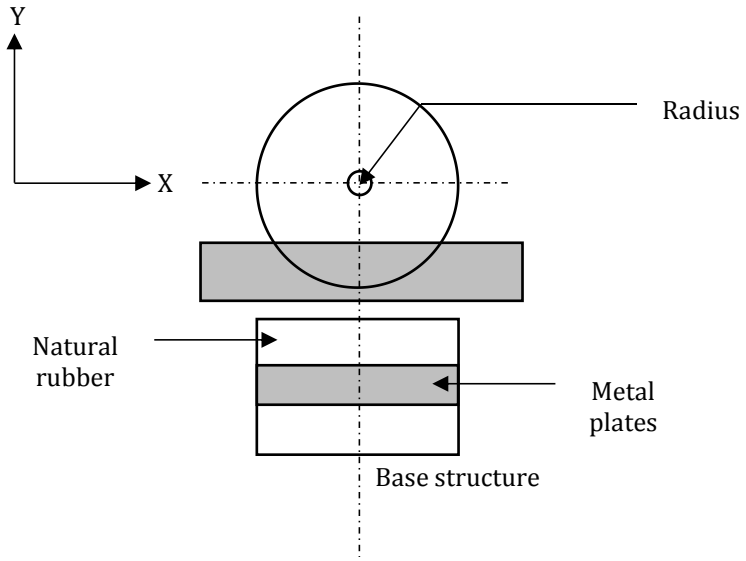

Figure 14. Basic elements in a laminated rubber-metal spring.

In this section, the derivation of one-dimensional elements of the non-dispersive finite rod due to transmissibility plots has been developed. One of the advantage of using this technique is the possibility to relate the dynamic behaviour of a finite structure or vibration isolators. On the other hand, this technique is particularly appropriate for highly damped systems and it can operate well in high frequency range.

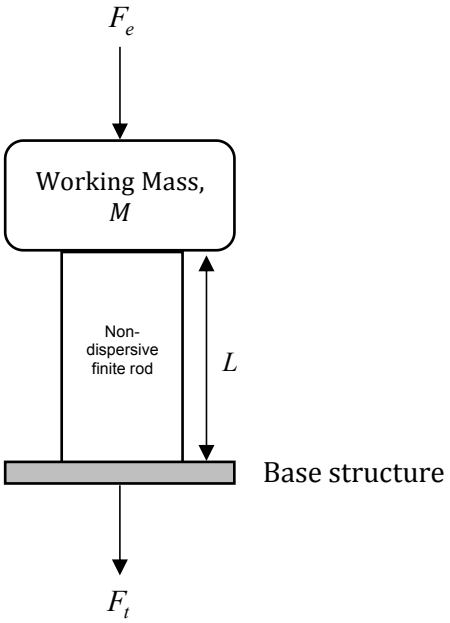

Figure 15. Working mass at the top of the non-dispersive finite rod.

4.2 Basic Assumptions of Isolator Model

Basically, the vibration isolator model can also be called as multilayer elastomeric bearings, in which composite elements consisting of natural rubber or synthetic rubber bonded and unbonded with metal plates. Additionally, it has the capability to withstand high compressive loads with some small longitudinal deformations. It is due to large bulk modulus of the rubber, and also a large shape factor from rubber layers. From literature, elastomeric bearing or isolator is widely used to isolate a high-rise building from ground-borne noise, prevent bridge from huge ocean wave and many more. Until today, there are thousands of buildings and bridges use rubber isolation to protect the vibration energy from earthquake, and most of these rubber bearings are in circular shape.

Vibration isolator is subjected to a combination of longitudinal loading and lateral displacement [14]. Then, the steel plate is not given any role in design process and it is generally considered as a rigid material in vibration isolator. But according to previous research by Ibrahim (2008), the vibration isolator bonded by metal plates usually has a high shape factor. It has a high ratio between loaded area to area free to bulge, and finally the applied stress becomes hydrostatic compression. Additionally, the maximum shear strain of the vibration isolator happens due to the combinatory effect of the compression loads and also the lateral displacement. Furthermore, the consistent measurement of the potential fatigue failure of the vibration isolator is also considered.

Design specification for vibration isolator recognizes these facts and also be considered in the design process. According to British Standard, an important criterion for design specification is focusing on the elongation at break of the vibration isolator. Furthermore, the dimension of the vibration isolator is important criteria in designing high performance isolator. British Standard has been adopted as a reference document in United State to design vibration isolator.

The British Standard that focuses on designing the vibration isolator is BE 1/76, and it is widely used as a reference to develop isolator. It expresses simple calculation of approximate theory for circular, and also for bonded isolator with metal plates in circular shape. However, this calculation is concentrated on simple analytical modelling in vertical loading. The new version of British Standard has been produced by adopting BE 1/76 which is called BS5400. In this new standard, it emphasizes about some assumptions that need to be made in designing the vibration isolator by using the previous approximate theory. Additionally, it also discusses the theory of bonded hollow circular vibration isolator.

4.3 Assumptions of the Basic Design

Natural rubber is a nonlinear and viscoelastic materials. To model the natural rubber as a vibration isolator, there are certain aspects that need to be considered because such modelling or prediction solution cannot be expressed in the form of nonlinear behaviour of the materials. According to this possibility, many researchers concluded that, nearly all analyses of vibration isolator in prediction methods are presumed linear, such as in the analysis of elasticity, isotropic behaviour and many more [14]. Even by having these assumptions, the prediction methods are still very difficult to solve for circular bonded vibration isolator. Therefore, some assumptions have been made by observing the physical reaction.

By considering an axisymmetric bonded vibration isolator (isolator bonded by metal plate at the middle of vibration isolator) subjected to small excitation force as shown in Figure 16 where F_e is excitation force, L is length, d is inner diameter, and D is outer diameter, then, the following assumption are made:

i. Vertical axis of deformation is presumed to have a parabolic shape or bulge, but it does not apply to metal plates.
ii. Any point of the vibration isolator is identified to have a normal stress and,
iii. Horizontal axis for vibration isolator remains as a plane

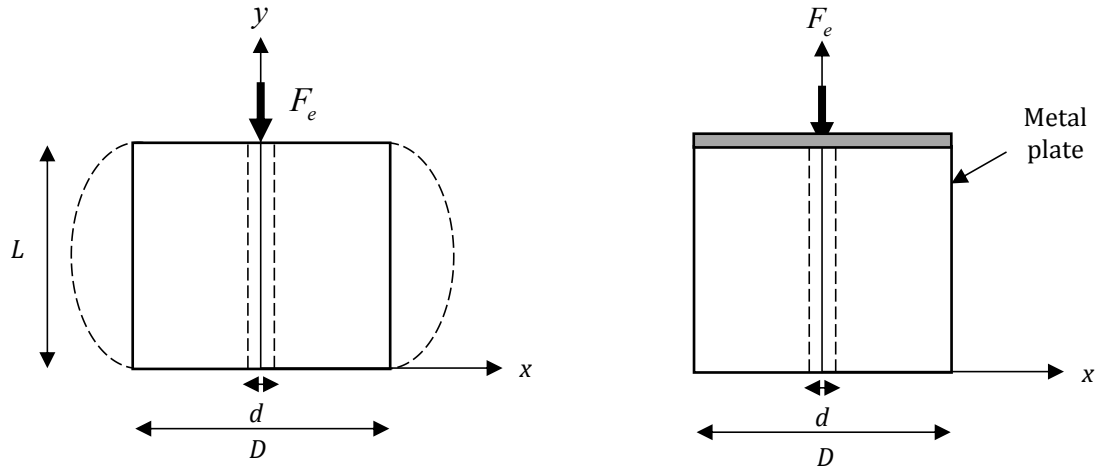

Figure 16. Vibration isolator subjected to small excitation force (a) unbonded by metal plate and (b) bonded by metal plate.

The normal stress of vibration isolator can be expressed by

$$\sigma_r = \sigma_y = -F_e(x) \tag{27}$$

Then, for an axisymmetric condition, it requires the shear stresses $\tau_{x\theta}$ and $\tau_{y\theta}$, where both of the equation represent the shear stress at x- and y-axis, respectively. Then, the displacement in the circumferential direction is presumed zero, $U_\theta = 0$. Another assumption results for radial displacement can be written as

$$U_x(x,y) = U_0(x)\left[1-\left(\frac{2y}{L}\right)^2\right] \tag{28}$$

where U_0 is the displacement at the middle of vibration isolator.

By considering the equilibrium of element of length, L, then the next assumption is made which is

$$\bar{\tau}_{xy} = -\frac{L}{2}\cdot\frac{dF_e}{dx} \tag{29}$$

where $\bar{\tau}_{xy}$ is the shear stress at the vibration isolator bonded with metal plate.

By using the constitutive relation, and then by utilizing the assumption and adopting Eq. (29), a new equation can be addressed by

$$U_0(x) = \frac{L^2}{8G}\cdot\frac{dF_e}{dx} \tag{30}$$

where G is the shear modulus of the vibration isolator.

Then, by taking the dilatational constitutive relationship in Eq. (3.27), the new assumption can be made and the equation can be written by

$$\frac{d^2F_e}{dx^2}+\frac{1}{x}\cdot\frac{dF_e}{dx}-\frac{12G}{L^2K}\cdot F_e = -\frac{12G}{L^2}\cdot\varepsilon \tag{31}$$

where K is bulk modulus and ε is compressive strain and boundary condition is $F_e = 0$ at the free surface.

Based on these assumptions, advanced research to study the individual errors had been carried out by Koh and Kelly methods (Constantinou *et al.*, 1992). Additionally, the prediction solutions obtained are used to verify the validity of incompressible materials, and it is accepted because the validity is reasonable and it can be used in designing vibration isolator (Sun and Zhang, 2013; Sun *et al.*, 2014).

4.4 Assumptions of the Circular Vibration Isolators

The prediction solutions for a circular vibration isolator have been recently discussed in previous section. In this section, it discusses specifically on circular vibration isolators assumption. It is very important and useful for presentation and discussion in the next section in order to derive the laminated rubber-metal spring model. Basically, the prediction solution of circular vibration isolator can be written as [15].

$$F_e(x) = K\varepsilon\left[1 - \frac{I_0\left(\beta x / R\right)}{I_0(\beta)}\right] \tag{32}$$

where I_0 is the modified Bessel function, and $\beta = S_f(48G/K)^2$, where S_f is the shape factor, and it can be defined as the loaded cross-sectional area divided by the area free to bulge, or in mathematical expression it can be given as $S_f = D/4L$.

By using the above equations, the shear stress at the bonded interface is derived with the maximum value of the shear strain, γ, and the expression is given by

$$\gamma = \frac{K\varepsilon\beta}{4GS} \cdot \frac{I_1(\beta)}{I_0(\beta)} \tag{33}$$

where I_1 is the modified Bessel function of order one.

If the value of β is too small and nearly to incompressible material, the expression in Eq. (33) can be rewritten as

$$\gamma \approx 6S\varepsilon - 36S^3 \cdot \left(\frac{G}{K}\right)\varepsilon \tag{34}$$

All of these equations have been verified by BS5400. In fact, the correlation of this assumptions have been verified with the specification in BE 1/76 and it is shown in Figure 3.16.

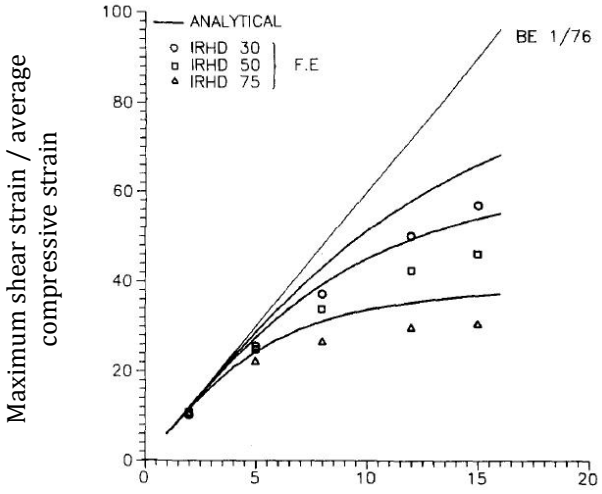

Figure 3.16. The correlation of the assumptions verified in BE 1/76 [15].

5. CONCLUSION

The aims of this paper is to develop the prediction tool for the basic and circular vibration isolator in high frequencies using the Malaysian natural rubber. At the end of the study, the aim

is achieved, which is the prediction tools is developed well. There are two techniques have been used which are lumped parameter system and wave propagation. The lumped parameters system basically focused on the baseline model of the vibration isolator which called as LR-MS in this study. Then, the wave propagation model has been developed using non-dispersive rod and it was elaborated well in this paper. The mathematical modelling which is a prediction tool hope it can have helped to predict the new methodology using trial-error method in future for developing new compounding of vibration isolator.

ACKNOWLEDGEMENTS

Special thanks to the Advanced Academia-Industry Collaboration Laboratory (AiCL) and Fakulti Kejuruteraan Mekanikal (FKM), Universiti Teknikal Malaysia Melaka (UTeM) for providing the laboratory facilities.

REFERENCES

[1] Y. Liu, W. Zhang, H. Yu, Z. Jing, Z. Song, and S. Wang, "A concise and antioxidative method to prepare copper conductive inks in a two-phase water/xylene system for printed electronics," *Chem. Phys. Lett.*, vol. **708**, (2018) pp.28–31.

[1] Shi, Y., Wu, P.D., Lloyd, D.J and Li, D.Y., "Effect of rate sensitivity on necking behavior of a laminated tube under dynamic loading", *Journal of Applied Mechanics, Transactions ASME*, Vol. **81**, No. 5, (2014) Art No. 051010.

[2] Imbimbo, M. and De Luca, A., F.E. "Stress analysis of rubber bearings under axial loads", *Computers and Structures*, Vol. **68**, (1998) pp.31-39.

[3] Manos, G. C., Mitoulis, S., Kourtidis, V., Sextos, A. and Tegos. I., "Study of the behavior of steel laminated rubber bearings under prescribed loads" *10th World Conference on Seismic Isolation, Energy Dissipation and Active Vibrations Control of Structures*, Istanbul, Turkey, (2007).

[4] Salim, M. A., Abdullah, M. A., & Putra, A., "Predicted transmissibility of an experimental approach for a laminated rubber-metal spring", *American-Eurasian Journal of Sustainable Agriculture*, (2014) pp.104-111.

[5] Salim, M. A., Putra, A., Thompson, D., Ahmad, N., & Abdullah, M. A., "Transmissibility of a laminated rubber-metal spring: A preliminary study". In *Applied Mechanics and Materials*, Vol. **393**, (2013) pp.661-665.

[6] Bhuiyan, A. R., Okui, Y., Razzak, M. K. and Amin, A. F. M. S., "earthquake resistant design of highway bridges using laminated rubber bearings: an approach for modeling hysteretic behavior based on experimental characteristic of rheology properties", *3rd International Earthquake Symposium*, Bangladesh, Dhaka, March 5-6, (2010) pp.381-389.

[7] Yan, B., Brennan, M.J., Elliott, S.J. and Ferguson, N.S., "Velocity feedback control of vibration isolation systems", *Technical Memorandum No. 962*. ISVR, University of Southampton, (2009).

[8] Ungar, E.E. and Dietrich, C.W., "High-frequency vibration isolation", *Journal of Sound and Vibration*, Vol. **4**, (1966) pp.224-241.

[9] Sykes, A.O., "Isolation of vibration when machine and foundation are resilient and when wave effects occur in the mount", *Noise Control*, Vol. **6**, No. 3, (1960) pp.115-130.

[10] Salim, M. A., Putra, A., Abdullah, M. A., & Ahmad, N., "Development of laminated rubber-metal spring using standard malaysian rubber constant viscosity-60", *International Review of Mechanical Engineering*, **8**, (2014) pp.761-765.

[11] Love, A. E. H., A Treatise on the Mathematical Theory of Elasticity, Dover, New York, 1944.

[12] Lin, H., Bengisu, T. and Mourelatos, Z., "Modeling the stiffness and damping of styrene-butadiene rubber", *SAE Technical Papers*, Code 91196, (2011).

[13] Lin, T. and Hone, C., "Base isolation by free rolling rods under basement", *Earthquake Engineering and Structural Dynamics*, Vol. **22**, (1993) pp.261–273.

[14] Ibrahim, R. A., "Recent advances in nonlinear passive vibration isolators", *Journal of Sound and Vibration*, Vol. **314**, (2008) pp.371-452.

[15] Constantinou, M. C., Juhn, G. and Manolis, G. D., "Stochastic response of secondary systems in base-isolated structures", *Probabilistic Engineering Mechanics,* **7**, (1992) pp.91-102.